ARTICLES
https://doi.org/10.1038/s41557-021-00789-w

nature chemistry

Prebiotic photoredox synthesis from carbon dioxide and sulfite

Ziwei Liu[1], Long-Fei Wu[1], Corinna L. Kufner[2], Dimitar D. Sasselov[2], Woodward W. Fischer[3] and John D. Sutherland[1]✉

Carbon dioxide (CO_2) is the major carbonaceous component of many planetary atmospheres, which includes the Earth throughout its history. Carbon fixation chemistry—which reduces CO_2 to organics, utilizing hydrogen as the stoichiometric reductant—usually requires high pressures and temperatures, and the yields of products of potential use to nascent biology are low. Here we demonstrate an efficient ultraviolet photoredox chemistry between CO_2 and sulfite that generates organics and sulfate. The chemistry is initiated by electron photodetachment from sulfite to give sulfite radicals and hydrated electrons, which reduce CO_2 to its radical anion. A network of reactions that generates citrate, malate, succinate and tartrate by irradiation of glycolate in the presence of sulfite was also revealed. The simplicity of this carboxysulfitic chemistry and the widespread occurrence and abundance of its feedstocks suggest that it could have readily taken place on the surfaces of rocky planets. The availability of the carboxylate products on early Earth could have driven the development of central carbon metabolism before the advent of biological CO_2 fixation.

Many carbon dioxide (CO_2) reduction reactions have been discussed in the context of prebiotic chemistry, but all are problematic in that they require very special conditions and/or materials that are simply rare on planetary surfaces. For example, reduction by the hydrogenation of bicarbonate (HCO_3^-) over a Ni–Fe alloy under hydrothermal conditions[1] requires high temperatures and pressures, and predominantly generates the C_1 product methane, a poor feedstock for elaboration into (proto) biomolecules. By separating H_2 and CO_2 with a thin Fe(Ni)S precipitate barrier across which there is a large pH difference, milder conditions enable the reduction, but the product formate (HCO_2^-) is only produced in trace amounts[2]. Reduction of CO_2 using metallic Fe powder in water generates acetate, methanol, formate and pyruvate—the latter only transiently—but the widespread occurrence of Fe powder on rocky planets, such as early Earth or Mars, is unlikely[3]. Finally, ultraviolet photoreduction of CO_2 on colloidal ZnS semiconductor particles using hydrogen sulfide/hydrosulfide (H_2S/HS^-) as a hole scavenger gives formate, acetate and propionate in low yields[4], but these conditions are not likely to be common in a planetary context.

We previously demonstrated that hydrogen cyanide can be reductively homologated using hydrated electrons (and/or hydrogen atoms derived therefrom by protonation) generated by ultraviolet irradiation of sulfidic anions in a process we termed cyanosulfidic chemistry[5,6]. For this chemistry, we originally used H_2S/HS^- as the stoichiometric reductant, but switched to bisulfite[7] (HSO_3^-, pK_a ~7.2)/SO_3^{2-} because sulfur dioxide (SO_2) and H_2S are outgassed in a ~10:1 or greater ratio on Earth[8,9], and there is substantial evidence from the geological records of both Earth and Mars via the anomalous mass fractionation of sulfur isotopes that these sulfur species were important constituents of the early sulfur cycle[10,11]. The Henry's law constant for SO_2 is greater than that for H_2S and the first pK_a of hydrated SO_2 (~1.9) is far lower than that of H_2S (~7.1) (ref. [12]), so the dissolution and hydration of SO_2 in surficial water followed by dissociation would therefore have been greater than the dissolution and dissociation of H_2S on early Earth and Mars. Based on reports that hydrated electrons generated by ultraviolet irradiation illuminating diamond surfaces reduce CO_2 to carbon monoxide (CO) in acidic aqueous solution[13], and the aforementioned semiconductor ultraviolet photoreduction of CO_2, we now wondered if HSO_3^-/SO_3^{2-} could serve as the source of hydrated electrons for CO_2 reduction by ultraviolet photodetachment[14] (Supplementary Table 1). Given that alkaline lakes can simultaneously absorb atmospheric CO_2 and SO_2 to give HCO_3^- and SO_3^{2-} and a growing body of evidence that suggests that such lakes could have concentrated other prebiotically important species on early Earth and maybe Mars[15,16], we started to explore reduction chemistry at mildly alkaline pH.

Results

Photoredox CO_2 fixation reaction. We subjected an aqueous solution of the sodium salts of HCO_3^- **1** (50 mM) and SO_3^{2-} (100 mM) at pH = 9 to ultraviolet irradiation from Hg lamps with a principal emission at 254 nm in a standard laboratory ultraviolet photoreactor and analysed the resultant mixture by ^{1}H NMR spectroscopy, integrating signals relative to those of a subsequently added standard to quantitate the products. After four hours irradiation, formate **2** (18 mM), hydroxymethanesulfonate **3** (200 μM), methanol **4** (200 μM), glycolate **5** (200 μM), acetate **6** (50 μM), tartronate **7** (600 μM) and malonate **8** (300 μM) were produced alongside both *rac*- and *meso*-tartrate **9a** (30 μM) and **9b** (30 μM) (the structures of the products are shown in Fig. 1 and Supplementary Fig. 1). Sulfate was detected as a photoredox co-product[14] by precipitation of barium sulfate on the addition of barium chloride under conditions in which barium sulfite is soluble[17]. The bicarbonate–sulfite irradiation experiment was repeated using ^{13}C-labelled HCO_3^- **1** to confirm that all the products were generated from the photoreduction of CO_2, and all the product assignments were confirmed by spiking with authentic standards (Supplementary Figs. 1 and 2). Surprisingly, we were able to detect elemental hydrogen (H_2) by ^{1}H NMR spectroscopy (δ = 4.5 ppm) if it was generated in situ by

[1]MRC Laboratory of Molecular Biology, Cambridge Biomedical Campus, Cambridge, UK. [2]Harvard-Smithsonian Center for Astrophysics, Massachusetts, MA, USA. [3]Division of Geological and Planetary Sciences, California Institute of Technology, Pasadena, CA, USA. ✉e-mail: johns@mrc-lmb.cam.ac.uk

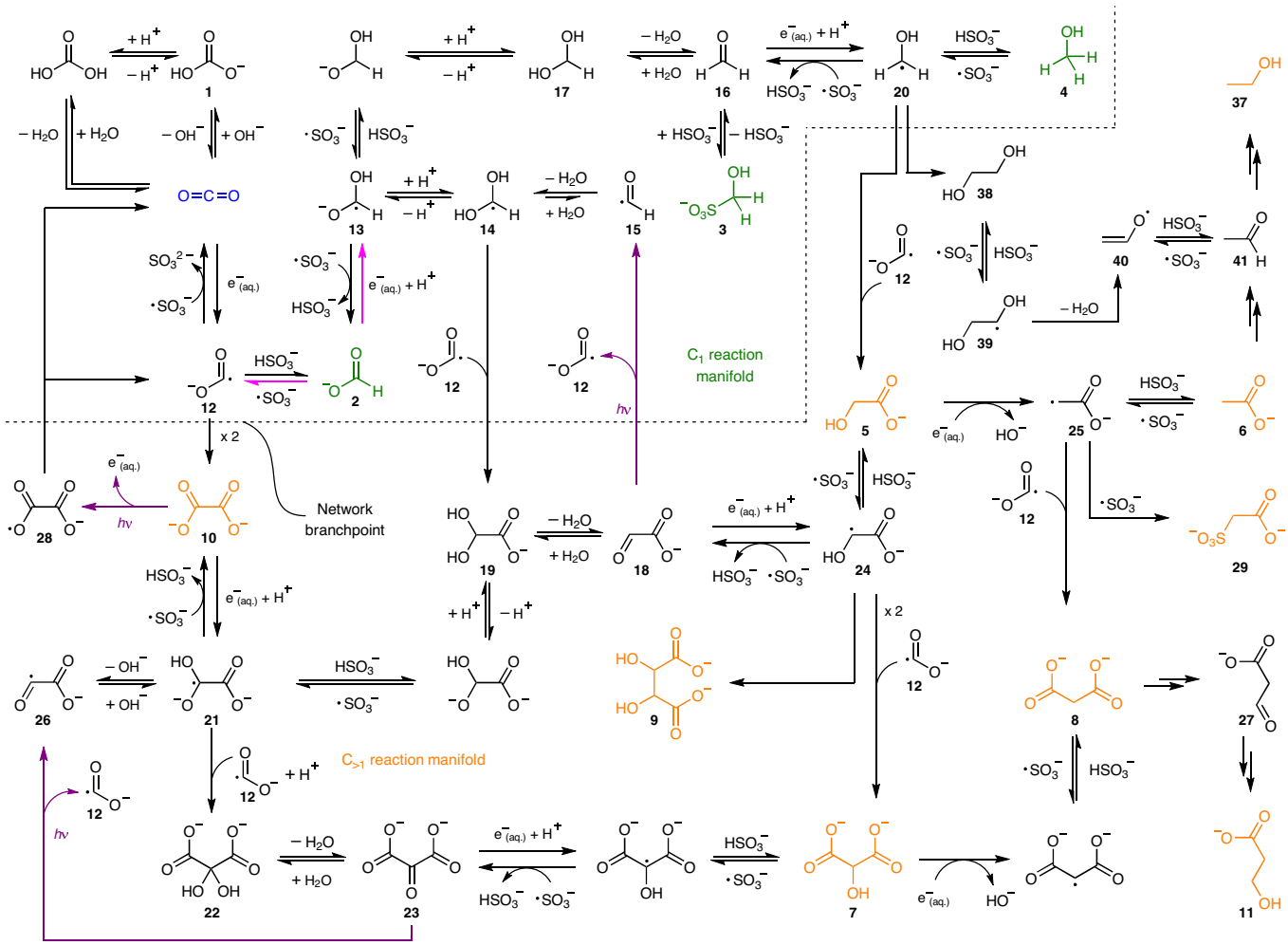

Fig. 1 | Carboxysulfitic photoredox reaction network starting from bicarbonate (HCO_3^-) 1. From the top left, the reaction network starts with the addition of hydrated electrons (produced by photodetachment from sulfite) to CO_2 (blue) to give the carboxyl radical **12** after which the network splits. Sequential reduction of the carboxyl radical **12** leads to the observed C_1 products (green), whereas dimerization of **12** to give oxalate **10** initiates a path to $C_{>1}$ products (orange). Various reactions enable crossing between the C_1 manifold and the $C_{>1}$ manifold (the two manifolds are separated by a dashed line). The key oxidation of formate **2** back to the carboxyl radical **12** and the slow reduction of **2** that together divert flux from the C_1 to $C_{>1}$ products are highlighted (fuchsia arrows). Photochemical reactions of oxalate **10**, glyoxylate **18** and mesoxalate **23** (purple arrows) also contribute to the network.

performing the irradiation experiment in a quartz NMR tube. This peak decreased and/or disappeared simply by shaking the NMR tube, presumably because this accelerated degassing. The signal assignment for H_2 was confirmed by running an NMR spectrum of the products of mixing zinc with hydrochloric acid solution in an NMR tube (Supplementary Fig. 3). Taken together, these results show that HCO_3^- **1** is reductively converted into C_2, C_3 and (traces of) C_4 compounds, as well as being reduced to other C_1 compounds in a process that also generates H_2 and SO_4^{2-}. If the initial concentration of HCO_3^- **1** was reduced to 5 mM and the concentration of SO_3^{2-} reduced to 10 mM, formate **2** (30 μM), glycolate **5** (20 μM), acetate **6** (10 μM), tartronate **7** (120 μM) and malonate **8** (30 μM) were observed by ^{1}H NMR spectroscopy after four hours of irradiation. The combined yield of organics in these experiments exceeded 10%, which demonstrates the remarkably high efficiency of this chemistry compared with that of other potentially prebiotic CO_2 fixation processes (Extended Data Fig. 1, entry 1, and Supplementary Fig. 4). The results were similar in experiments that started from CO_2 instead of sodium bicarbonate (Supplementary Fig. 5). In addition to the protiated products observed by ^{1}H NMR spectroscopy, oxalate **10** was observed by ^{13}C NMR spectroscopy in yields as high as 11% (Supplementary Fig. 6). At higher concentrations of reactants, the yield of C_1 products, especially formate **2**, went up relative to the yield of $C_{>1}$ products and after prolonged irradiation, a new C_3 product, β-hydroxypropionate **11**, was identified (Extended Data Fig. 1, entries 2–5, Supplementary Fig. 7).

Mechanistic study of the photoredox CO_2 fixation reaction network. We next investigated the photoreaction of the various products and some putative intermediates in the presence of SO_3^{2-} with a view to gaining information about the mechanism of the fixation chemistry. The results—summarized in Extended Data Fig. 2 (Supplementary Figs. 8–19)—can be rationalized by a reaction network based on photoredox radical chemistry (Fig. 1). Photodetachment of an electron from SO_3^{2-} gives a hydrated electron and a sulfite radical ($SO_3^{\cdot-}$) (ref. [14]). At pH 9, both the loss of hydroxide from HCO_3^- **1** and the loss of water from its conjugate acid, H_2CO_3, furnish CO_2. The latter process is efficiently catalysed by nucleophiles[18–20], especially sulfite[21], so it is unlikely that the otherwise slow kinetics of equilibration limit the photoredox chemistry. Although the equilibrium concentration of CO_2 is very low in a solution that contains HCO_3^- **1** at pH = 9 relative to the concentration of **1** (Supplementary Fig. 20a)[22], the rate constant for the reaction of CO_2 with hydrated electrons to give the carboxyl radical

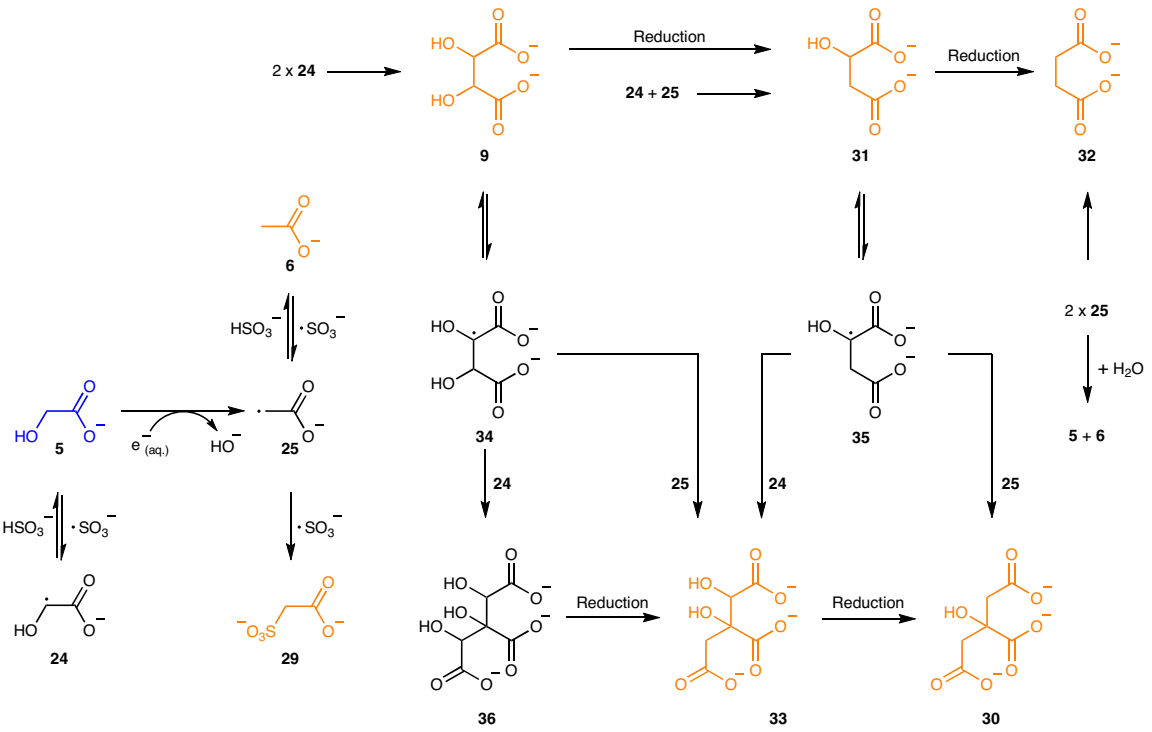

Fig. 2 | Carboxysulfitic photoredox reaction network starting from glycolate 5. Glycolate **5** (blue) can be both oxidized by sulfite radicals and reduced by hydrated electrons to give the radicals **24** and **25**, which then react further to give the observed products (orange). Recombination of two C_2 radicals (**24** and/or **25**) gives C_4 products (tartrate **9**, malate **31** and succinate **32**). Tartrate **9** and malate **31** can be oxidized by sulfite radicals to give C_4 radicals **34** and **35** and the recombination of C_2 and C_4 radicals gives C_6 compounds (including the products hydroxycitrate **33** and citrate **30**). The reduction of dihydroxycitrate **36** and tartrate **9** provides additional reaction pathways to the C_6 and other C_4 products.

12 is extremely high[23] and the rate greatly exceeds that for the protonation of hydrated electrons by **1** to give hydrogen atoms[24]. The carboxyl radical **12** can either be reduced by hydrogen atom transfer (HAT) from HSO_3^-, which has an about 1% abundance relative to that of SO_3^{2-} at pH = 9, to give formate **2**, or undergo dimerization to give oxalate **10**, both directly and indirectly[25]. Focussing on the chemistry of formate **2** first, a one-electron reduction, although relatively slow[26], gives the radical anion **13** and thence, through acid–base and hydration equilibria, the radicals **14** and **15** (although the latter is unfavoured relative to **13** and **14**). The radicals **13** and **14** have two main fates—reduction by HAT from HSO_3^- or recombination with the carboxyl radical **12**. Coupled with acid–base and hydration equilibria, the first process (shown only for **13**), generates formaldehyde **16** and its hydrate **17**, and the second (shown only for **14**) generates glyoxylate **18** via its hydrate **19**. Formaldehyde **16**, in equilibrium with the bisulfite adduct **3**, can be reduced to the radical **20**, which gives methanol **4** by HAT and glycolate **5** by recombination with the carboxyl radical **12**[27]. Another major reaction of formate **2** is oxidation back to carboxyl radical **12** by reaction with sulfite radicals. This is inferred from the observation that irradiation of formate **2** and SO_3^{2-} gives moderate amounts of what appear to be products that derive from oxalate **10** in addition to C_1 products (Extended Data Fig. 2).

The other initial product of the carboxyl radical **12**—its dimer oxalate **10**—can be reduced by the addition of a hydrated electron to give the radical anion **21**[28]. This reduction is much faster than the corresponding reduction of formate **2** (ultrafast pump–probe experiments and discussion are given in Methods). The radical anion **21** can undergo HAT, which leads to glyoxylate hydrate **19**, or recombination with another carboxyl radical **12** to give mesoxalate hydrate **22**, which equilibrates with mesoxalate **23**[29]. Reduction of mesoxalate **23** by the addition of a hydrated electron, or electron transfer from a carboxyl radical **12**, followed by HAT gives tartronate **7** and deoxygenation of the latter followed by HAT gives malonate **8**. In the same multistep way that formate **2** can be reduced to methanol **4**, the reduction of one of the carboxylate groups of malonate **8** leads to β-hydroxypropionate **11**. Reduction of glyoxylate **18** (in equilibrium with the hydrate **19** and a bisulfite adduct)[30] and protonation of the initially formed radical anion[31] leads to the key hydroxy–carboxymethyl radical **24** ($pK_a \approx 8.8$) (ref. [32]), which can recombine with the carboxyl radical **12** to give tartronate **7**, dimerize to give the tartrates **9** or undergo HAT to give glycolate **5**. Deoxygenation of glycolate **5** gives the carboxymethyl radical **25**, which by recombination with the carboxyl radical **12** can give malonate **8**[33] and, by HAT, acetate **6**.

Finally, we identified a number of photochemical steps other than the photodetachment of electrons from SO_3^{2-} that initiate the reaction network. Norrish type I reactions of glyoxylate **18** and mesoxalate **23** generate radicals **12**, **15** and **26** (a similar photocleavage of malonsemialdehyde **27**, en route to β-hydroxypropionate **11**, would generate radicals **15** and **25**) and photodetachment of an electron from oxalate **10**[34,35] gives radical **28**, which is thought to decarboxylate to the carboxyl radical **12**. These additional photochemical steps set up futile cycles in the network, but also forge links from the $C_{>1}$ parts of the network to the C_1 part (Supplementary Figs. 21–26).

Based on the foregoing analysis, we thought that it might be possible to increase the amount of the $C_{>1}$ products by adding sulfite portionwise, which would ensure that, at any one time, the concentration of HSO_3^- would be low, so the reaction flux through oxalate **10** would be favoured, but overall there would be more reduction capacity. In accordance with expectation, at the end of this experiment, the combined yield of $C_{>1}$ products (>25%) greatly exceeded

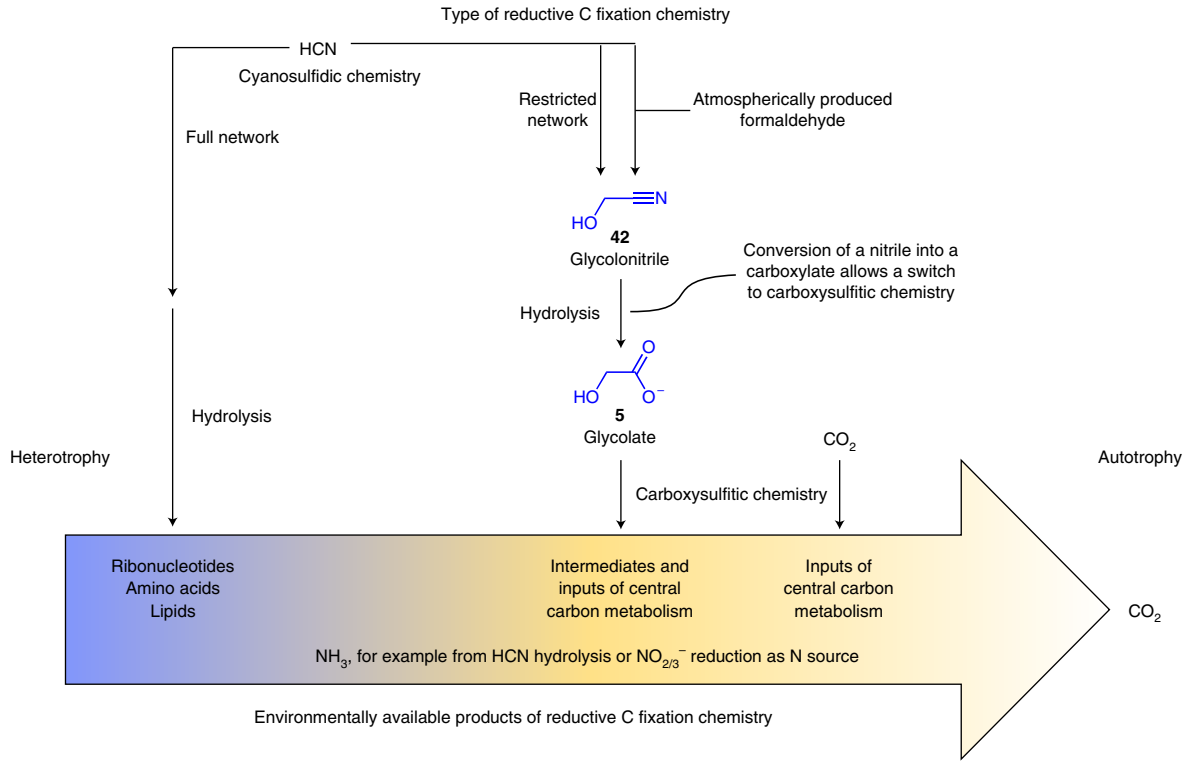

Fig. 3 | Connections between environmental chemistry and the development of metabolism. Progression from heterotrophy fed by the photochemical products of inorganic carbon reduction to autotrophy as the available products of environmental chemistry become less complex. The preformed building blocks of RNA, peptides and lipids produced by cyanosulfidic chemistry provision the origin and early evolution of life[5,54], but gradually become depleted (fading of the blue colour in the timeline arrow), which triggers the development of metabolism starting from simpler, but more abundant, products derived from glycolate **5** by cyanosulfidic chemistry (dark orange in the timeline arrow). In turn, these materials become scarce (fading of the orange colour in the timeline arrow) and biology adapts to using carboxysulfitic products of CO_2 and, eventually, CO_2 itself.

that of C_1 products (<1%) and the combined yield of malonate **8** (16.2%) and acetate **6** (1.0%) was greater than twice that of tartronate **7** (6.6%) and glycolate **5** (0.8%). Unexpectedly, a new product, sulfoacetate **29** (0.8%) was formed in low yield, presumably through recombination of carboxymethyl radicals **25** with sulfite radicals (Extended Data Fig. 1, Entry 6, and Supplementary Fig. 27). The general features of the time course of the CO_2 reduction network were also revealed by this experiment. After one hour, formate **2** was the major product accompanied by traces of glycolate **5** and tartronate **7**. After two hours, the amount of formate **2** had decreased and glycolate **5** and tartronate **7** became the major products, along with smaller amounts of acetate **6** and malonate **8**. After further irradiation, the levels of formate **2**, glycolate **5** and tartronate **7** stayed about the same and malonate **8** became the major product with minor amounts of acetate **6** and methanol **4**. This time-course behaviour can be understood from the reaction network (Fig. 1). At the outset of the experiment, the only carbonaceous species for the hydrated electrons to reduce is CO_2. Carboxyl radicals **12** thereby produced apparently undergo HAT from HSO_3^- faster than they dimerize, and so formate **2** increases. However, the conversion of carboxyl radicals **12** to give **2** is reversible, and so after some time a sufficient amount of oxalate **10** is produced for it to be reduced by the hydrated electrons as well. The reduction of oxalate **10** is much faster than that of formate **2** (investigated by ultrafast pump–probe spectroscopy and further discussed in Methods), so **2** is consumed at the expense of making reduction products of **10**. The appearance of the radical anion **21** opens up a new path for the consumption of carboxyl radicals **12**, which includes recombination to give mesoxalate hydrate **22**, which is rapidly converted into tartronate **7** and gives a new path for the consumption of HSO_3^-, namely HAT to **21** to give glyoxylate **18** and thence, through rapid further reduction, glycolate **5**. The opening of these new reaction paths reduces the level of formate **2** to a steady state at which its consumption is balanced by continuous production from CO_2 via carboxyl radicals **12**. Eventually, the deoxygenation of tartronate **7** coupled to the slow reduction of malonate **8** means that the latter becomes the predominant product. At higher initial concentrations of sulfite, the early formate **2** pulse lasts longer and produces higher early amounts of **2**, but eventually the paths to $C_{>1}$ products start to operate and levels of formate **2** drop. Even if formate **2** is reduced, the reversibility of the downstream steps to C_1 products and other paths from the C_1 part of the network to the $C_{>1}$ part means that products more complex than **2** eventually accumulate.

It has been reported that CO_2 can be reduced to CO with hydrated electrons produced by the ultraviolet irradiation of diamond in the presence of bisulfite as a hole scavenger at pH = 3.2 (ref. [13]). The carboxyl radical **12** is formed as in our chemistry, but without the chromophoric sulfite that acts to absorb ultraviolet, it is photolysed[36] to CO and $O^{\bullet-}$, the conjugate base of the hydroxyl radical, which is then reduced by bisulfite. Hydrogen was not observed as a product because the reaction was carried out under a sufficiently high concentration of CO_2 to outcompete H^+ in reactions with electrons.

Glycolate photoredox reaction. As we investigated the photoreactions of the products and putative intermediates of the CO_2 reduction network with SO_3^{2-}, the photoredox chemistry of one product—glycolate **5**—stood out. Acetate **6** (16.2 mM), malonate **8** (0.1 mM), sulfoacetate **29** (7.8 mM), citrate **30** (0.2 mM), tartronate **7**, *rac*-tartrate **9a** (1.5 mM, the total amount of **7** and **9a**), *meso*-tartrate

9b (1.0 mM), malate **31** (2.9 mM), succinate **32** (1.1 mM) and hydroxycitrate **33** (0.19 mM), along with C_1 products, were detected by ^{1}H NMR spectroscopy after six hours of irradiation of glycolate **5** (50 mM) and SO_3^{2-} (100 mM) (Extended Data Fig. 2, Entry 4, and Supplementary Fig. 12). Particularly noteworthy is the fact that citrate **30**, malate **31** and succinate **32** are key constituents of the Krebs cycle—a major cycle of central carbon metabolism, the consequences of which are discussed below. Remarkably, when the concentration of glycolate **5** was reduced to 5 mM and the concentration of SO_3^{2-} reduced to 10 mM, after two hours of irradiation, C_1 products were no longer detected but the higher products were still formed in a comparable overall yield, albeit with a different relative abundance distribution (Extended Data Fig. 2, Entry 5, and Supplementary Fig. 13). The chemistry that generates acetate **6**, malonate **8** and the tartrates **9** is the same as some of that for the CO_2 fixation reaction network, but additional reactions now contribute to the detectable products (Fig. 2). Abstraction of a hydrogen atom from glycolate **5** by a sulfite radical generates the hydroxycarboxymethyl radical **24**, whereas the redox compensatory reduction of **5** generates the carboxymethyl radical **25**. Dimerization of **24** produces the tartrates **9**, whereas dimerization of **25** produces succinate **32**, as well as acetate **6** and glycolate **5**[37]. Recombination of radicals **24** and **25** provides one route to malate **31**, a second would be from the reduction of **9**. Similar reduction of malate **31** would give a second path to succinate **32**. Oxidation of the tartrates **9** and malate **31** to give the corresponding hydroxyalkyl radicals **34** and **35** followed by recombination of these radicals with radicals **24** or **25** would give dihydroxycitrate **36**, hydroxycitrate **33** and citrate **30**. Reduction of **36** would constitute another reaction channel to hydroxycitrate **33** and further reduction of **33**, another channel to citrate **30**. In contrast with the reaction network starting from CO_2, in which all the products are reduced relative to the starting material, the network starting from glycolate **5** is more subtle and contains both carbon oxidations and reductions. Thus, malate **31** and citrate **30** are at the same oxidation level as glycolate **5**, succinate **32** and acetate **6** are more reduced and the tartrates **9** and hydroxycitrate **33** are, on average, more oxidized.

Photoredox reactions under a lower photon flux. We also evaluated the bicarbonate reduction chemistry using a less-intense broadband ultraviolet source, StarLab[38]—an in-house constructed photoreactor designed to deliver ultraviolet radiation with a wavelength distribution representative of that from the Sun incident on the surface of early Earth, at a ~100-fold higher intensity than the Sun in a quiescent state and ~10-fold lower intensity than that during maximum flaring. After irradiation for seven days in this apparatus, an aqueous solution of the sodium salts of HCO_3^- **1** (5 mM) and SO_3^{2-} (50 mM) at pH = 9 gave a mixture of protiated products similar to that obtained on a higher intensity irradiation in the standard laboratory photoreactor (at 254 nm for shorter time intervals) plus ethanol **37**, which confirms the utility of using 254 nm ultraviolet light to study this chemistry (Extended Data Fig. 1, Entry 7, and Supplementary Fig. 28). Oxalate **10** was also detected in a similar experiment using the ^{13}C-labelled bicarbonate (Supplementary Fig. 29). Ethanol **37** could plausibly be obtained via dimerization of the hydroxymethyl radical **20** to give ethylene glycol **38**, dehydration of **38** through radical **39** and the enoloxy radical **40**[39] to acetaldehyde **41** and reduction (Fig. 1). Alternatively, acetate **6** could be reduced to acetaldehyde **41** and thence ethanol **37**.

We then investigated the carboxysulfitic photoredox chemistry of glycolate **5** in the StarLab photoreactor. After eight hours irradiation of glycolate **5** (50 mM) and SO_3^{2-} (100 mM) with this less-intense light source, acetate **6** (1.7 mM), sulfoacetate **29** (0.2 mM), tartronate **7**, *rac*-tartrate **9a** (0.4 mM, the total amount of **7** and **9a**), *meso*-tartrate **9b** (0.4 mM), malate **31** (0.2 mM) and succinate **32** (trace) along with C_1 products were detected by ^{1}H NMR spectroscopy (Extended Data Fig. 2, Entry 6, and Supplementary Fig. 14). Longer irradiation of more dilute samples of glycolate **5** (5 mM) and SO_3^{2-} (50 mM) in the StarLab photoreactor resulted in higher yields of the same species and additionally produced malonate **8** and hydroxypropionate **11** (Extended Data Fig. 2, Entry 7, and Supplementary Fig. 30).

Discussion

Planetary relevance. An important aspect of this chemistry is that the conditions and materials necessary to foster carboxysulfitic carbon fixation (short-wave ultraviolet light, CO_2 and SO_2 derived from volcanism, and bodies of standing and flowing water on the crust) are mild, widespread and expected to be common on rocky planets. Notably, there is geological evidence from the rock records of Earth and Mars that these conditions were met early in their history. Oxygen isotope ratios from Hadean zircons[40,41] and sedimentological observations from the earliest sedimentary record[42] indicate abundant surface liquid water. Silicate weathering reactions occurred that sourced the alkalinity necessary to enable the dissociated hydrates, bicarbonate and sulfite to partition from the atmosphere and accumulate in bodies of water in contact with the atmosphere[43]. Moreover, the anomalous fractionation of multiple sulfur isotopes in the early geological record[10] provides a direct measure of SO_2 photochemistry, which establishes a valuable atmospheric correlate of the aqueous carbon fixation processes described herein. Finally, each of these observations for the early Earth that illustrates the plausibility of this chemistry occurring now has its complement in the Mars geological record[11,44–47]. Thus, the ingredients and basic conditions for carboxysulfitic chemistry to take place would have been present on both Earth and Mars. Depending on the conditions, carboxylates such as formate **2**, oxalate **10** or acetate **6** and malonate **8** are likely to have been the major initial products. Decarboxylation of malonate **8** to give acetate **6** occurs on a short geological timescale in solution (about ten years at neutral pH and 25 °C) (ref. [48]), whereas oxalate **10** (in the absence of ferric ions and light)[49], like acetate **6**, is long-term stable and so it seems likely that these latter two products would have become the most abundant $C_{>1}$ organics on early Earth had life not emerged—they might still be the most abundant organics on Mars if life did not emerge there.

The linkage between carboxysufitic chemistry and cyanosulfidic chemistry. The case for conditions conducive to cyanosulfidic chemistry being present on both young planets has also been made[50]. We note that for the full range of cyanosulfidic chemistry products to result, a scenario that involves the mixing of bodies of water or flows (for example, stream water) with subtly different reaction histories would probably be necessary. In locations where the basic conditions for cyanosulfidic chemistry were met, but the mixing of streams was absent or different, a limited set of products would have been generated and the first product of the restricted reaction network, glycolonitrile **42**, would probably have been the most widespread. In addition, glycolonitrile **42** could have resulted from the reaction of hydrogen cyanide with formaldehyde **16** rained in after production in the upper atmosphere by the photoreduction of CO_2 (ref. [51]). Hydrolysis of the nitrile group of glycolonitrile **42**, however produced, generates glycolate **5**, which could be converted by subsequent carboxysulfitic chemistry into the range of carboxylate products previously described (Fig. 3). As the hydrolysis of glycolonitrile **42** generates ammonia in addition to glycolate **5**, we also carried out the irradiation of **5** and sulfite in the presence of ammonia. Ammonia did not affect the outcome of the photoredox chemistry–the same set of products was formed with or without ammonia (Supplementary Fig. 31).

Biochemical relevance. Use of the products of cyanosulfidic chemistry as building blocks by nascent biology would eventually lead

to their environmental depletion and biology would then be under evolutionary pressure to synthesize these building blocks from anything else that happened to be available and usable. Biology could either spread to encounter these materials in their place of synthesis, or fluvial advection could move them to the location of biology. It is fascinating that the majority of the carboxylate products that derive from the carboxysulfitic chemistry of glycolate **5** are key nodes of central carbon metabolism in extant biology and it seems likely that their synthesis by carboxysulfitic chemistry set the stage for the development of this metabolic network. At first glance, tartrate **9** seems to be somewhat an outlier, but its dehydration would lead through an enol to oxaloacetate[52] and its oxidation to dihydroxyfumarate, which spontaneously decarboxylates to give glycolaldehyde[53], a precursor of higher sugars.

With time, the supply of most of the products of the carboxysulfitic chemistry of glycolate **5** would also dwindle and biology would have to evolve to make do with simpler, more abundant carbonaceous materials in the environment. The major long-term stable products of the carboxysulfitic chemistry of CO_2—formate **2**, acetate **6** and oxalate **10**—could then provision central carbon metabolism through the development of a pyruvate–formate lyase activity and the glyoxylate shunt of the Krebs cycle via the reduction of oxalate **10** to give glyoxylate **18**. Finally, even oxalate **10** and acetate **6** would become depleted and biology would be under evolutionary pressure to use the only remaining abundant carbon source, namely CO_2.

Online content

Any methods, additional references, Nature Research reporting summaries, source data, extended data, supplementary information, acknowledgements, peer review information; details of author contributions and competing interests; and statements of data and code availability are available at https://doi.org/10.1038/s41557-021-00789-w.

Received: 2 February 2021; Accepted: 17 August 2021;
Published online: 11 October 2021

References

1. Horita, J. & Berndt, M. E. Abiogenic methane formation and isotopic fractionation under hydrothermal conditions. *Science* **285**, 1055–1057 (1999).
2. Hudson, R. et al. CO_2 reduction driven by a pH gradient. *Proc. Natl Acad. Sci. USA* **117**, 22873–22879 (2020).
3. Varma, S. J., Muchowska, K. B., Chatelain, P. & Moran, J. Native iron reduces CO_2 to intermediates and end-products of the acetyl-CoA pathway. *Nat. Ecol. Evol.* **2**, 1019–1024 (2018).
4. Zhang, X. V. et al. Photodriven reduction and oxidation reactions on colloidal semiconductor particles: implications for prebiotic synthesis. *J. Photochem. Photobiol. Chem.* **185**, 301–311 (2007).
5. Patel, B. H., Percivalle, C., Ritson, D. J., Duffy, C. D. & Sutherland, J. D. Common origins of RNA, protein and lipid precursors in a cyanosulfidic protometabolism. *Nat. Chem.* **7**, 301–307 (2015).
6. Green, N. J., Xu, J. & Sutherland, J. D. Illuminating life's origins: UV photochemistry in abiotic synthesis of biomolecules. *J. Am. Chem. Soc.* **143**, 7219–7236 (2021).
7. Xu, J. et al. Photochemical reductive homologation of hydrogen cyanide using sulfite and ferrocyanide. *Chem. Commun.* **54**, 5566–5569 (2018).
8. Zahnle, K., Claire, M. & Catling, D. The loss of mass-independent fractionation in sulfur due to a Palaeo-proterozoic collapse of atmospheric methane. *Geobiology* **4**, 271–283 (2006).
9. Gerlach, T. M. Evaluation and restoration of the 1970 volcanic gas analyses from Mount Etna, Sicily. *J. Volcanol. Geotherm. Res.* **6**, 165–178 (1979).
10. Farquhar, J., Bao, H. & Thiemens, M. Atmospheric influence of Earth's earliest sulfur cycle. *Science* **289**, 756–758 (2000).
11. Farquhar, J., Savarino, J., Jackson, T. & Thiemens, M. H. Evidence of atmospheric sulphur in the Martian regolith from sulphur isotopes in meteorites. *Nature* **404**, 50–52 (2000).
12. Ranjan, S., Todd, Z. R., Sutherland, J. D. & Sasselov, D. D. Sulfidic anion concentrations on early earth for surficial origins-of-life chemistry. *Astrobiology* **18**, 1023–1040 (2018).
13. Zhang, L., Zhu, D., Nathanson, G. M. & Hamers, R. J. Selective photoelectrochemical reduction of aqueous CO_2 to CO by solvated electrons. *Angew. Chem. Int. Ed.* **126**, 9904–9908 (2014).
14. Fischer, M. & Warneck, P. Photodecomposition and photooxidation of hydrogen sulfite in aqueous solution. *J. Phys. Chem.* **100**, 15111–15117 (1996).
15. Toner, J. D. & Catling, D. C. A carbonate-rich lake solution to the phosphate problem of the origin of life. *Proc. Natl Acad. Sci. USA* **117**, 883–888 (2020).
16. Toner, J. D. & Catling, D. C. Alkaline lake settings for concentrated prebiotic cyanide and the origin of life. *Geochim. Cosmochim. Acta* **260**, 124–132 (2019).
17. Malati, M. A. *Experimental Inorganic/Physical Chemistry: an Investigative, Integrated Approach to Practical Project Work* (Woodhead, 1999).
18. Murphy, L. J. et al. A simple complex on the verge of breakdown: isolation of the elusive cyanoformate ion. *Science* **344**, 75–78 (2014).
19. Hering, C., von Langermann, J. & Schulz, A. The elusive cyanoformate: an unusual cyanide shuttle. *Angew. Chem. Int. Ed.* **53**, 8282–8284 (2014).
20. Juhl, M., Petersen, A. R. & Lee, J.-W. CO_2-enabled cyanohydrin synthesis and facile iterative homologation reactions. *Chem. Eur. J.* **27**, 228–232 (2021).
21. Roughton, F. J. W. & Booth, V. H. The catalytic effect of buffers on the reaction $CO_2 + H_2O = H_2CO_3$. *Biochem. J.* **32**, 2049–2069 (1938).
22. Zeebe, R. E., & Wolf-Gladrow, D. *CO_2 in Seawater: Equilibrium, Kinetics, Isotopes* (Gulf Professional, 2001).
23. Gordon, S., Hart, E. J., Matheson, M. S., Rabani, J. & Thomas, J. K. Reactions of the hydrated electron. *Discuss. Faraday Soc* **36**, 193–205 (1963).
24. Hentz, R. R., Farhataziz, Milner, D. J. & Burton, M. γ-Radiolysis of liquids at high pressures. III. Aqueous solutions of sodium bicarbonate. *J. Chem. Phys.* **47**, 374–377 (1967).
25. Flyunt, R., Schuchmann, M. N. & von Sonntag, C. A common carbanion intermediate in the recombination and proton-catalysed disproportionation of the carboxyl radical anion $CO_2^{\cdot-}$ in aqueous solution. *Chem. Eur. J.* **7**, 796–799 (2001).
26. Swallow, A. J. Recent results from pulse radiolysis. *Photochem. Photobiol.* **7**, 683–694 (1968).
27. Getoff, N., Gütlbauer, F. & Schenck, G. O. Strahlenchemische carboxylierung von ameisensäure und methanol in wässriger lösung. *Int. J. Appl. Radiat. Isot.* **17**, 341–349 (1966).
28. Getoff, N., Schwörer, F., Markovic, V. M., Sehested, K. & Nielsen, S. O. Pulse radiolysis of oxalic acid and oxalates. *J. Phys. Chem.* **75**, 749–755 (1971).
29. Doussin, J.-F. & Monod, A. Structure–activity relationship for the estimation of OH-oxidation rate constants of carbonyl compounds in the aqueous phase. *Atmos. Chem. Phys.* **13**, 11625–11641 (2013).
30. Olson, T. M. & Hoffmann, M. R. Formation kinetics, mechanism and thermodynamics of glyoxylic acid–S(IV) adducts. *J. Phys. Chem.* **92**, 4246–4253 (1988).
31. Laroff, G. P. & Fessenden, R. W. ^{13}C hyperfine interactions in radicals from some carboxylic acids. *J. Chem. Phys.* **55**, 5000–5008 (1971).
32. Bell, J. A., Grunwald, E. & Hayon, E. Kinetics of deprotonation of organic free radicals in water. Reaction of $HOC{\cdot}HCO_2^{-}$, $HOC{\cdot}HCONH_2$ and $HOC{\cdot}CH_3CONH_2$ with various bases. *J. Am. Chem. Soc.* **97**, 2995–3000 (1975).
33. Getoff, N. CO_2 and CO utilization: radiation-induced carboxylation of aqueous chloroacetic acid to malonic acid. *Radiat. Phys. Chem.* **67**, 617–621 (2003).
34. Arvis, M., Lustig, H. & Hickel, B. Étude par photolyse éclair de la photoionisation des anions formiate, acetate et oxalate dans l'eau. *J. Photochem.* **13**, 223–232 (1980).
35. Huie, R. E. & Clifton, C. L. Kinetics of the reaction of the sulfate radical with the oxalate anion. *Int. J. Chem. Kinet.* **28**, 195–199 (1996).
36. Habteyes, T., Velarde, L. & Sanov, A. Photodissociation of CO_2^{-} in water clusters via Renner–Teller and conical interactions. *J. Chem. Phys.* **126**, 154301 (2007).
37. Wang, W.-F., Schuchmann, M. N., Schuchmann, H.-P. & von Sonntag, C. The importance of mesomerism in the termination of α-carboxymethyl radicals from aqueous malonic and acetic acids. *Chem. Eur. J.* **7**, 791–795 (2001).
38. Rimmer, P. et al. Timescales for prebiotic photochemistry under realistic surface UV conditions. *Astrobiology* https://doi.org/10.1089/ast.2020.2335 (in the press).
39. Gilbert, B. C., Larkin, J. P. & Norman, R. O. C. Electron spin resonance studies. Part XXXIII. Evidence for heterolytic and homolytic transformations of radicals from 1,2-diols and related compounds. *J. Chem. Soc. Perkin Trans. 2* **1972**, 794–802 (1972).
40. Wilde, S., Valley, J., Peck, W. & Graham, C. M. Evidence from detrital zircons for the existence of continental crust and oceans on the Earth 4.4 Gyr ago. *Nature* **409**, 175–178 (2001).
41. Valley, J. W. et al. 4.4 billion years of crustal maturation: oxygen isotope ratios of magmatic zircon. *Contrib. Mineral. Petrol.* **150**, 561–580 (2005).
42. Rosing, M. T. ^{13}C-depleted carbon microparticles in >3700-Ma sea-floor sedimentary rocks from west Greenland. *Science* **283**, 674–676 (1999).
43. Kasting, J. F. The Goldilocks planet? How silicate weathering maintains Earth 'just right'. *Elements: Int. Mag. Mineral. Geochem. Petrol.* **15**, 235–240 (2019).
44. Grotzinger, J. P. et al. Deposition, exhumation, and paleoclimate of an ancient lake deposit, Gale crater, Mars. *'Science* **350**, aac7575 (2015).

45. DiBiase, R. A., Limaye, A. B., Scheingross, J. S., Fischer, W. W. & Lamb, M. P. Deltaic deposits at Aeolis Dorsa: sedimentary evidence for a standing body of water on the northern plains of Mars. *J. Geophys. Res. Planets* **118**, 1285–1302 (2013).
46. Hurowitz, J. A. Redox stratification of an ancient lake in Gale Crater, Mars. *Science* **356**, eaah6849 (2017).
47. Milliken, R. E., Fischer, W. W. & Hurowitz, J. A. Missing salts on early Mars. *Geophys. Res. Lett.* **36**, L11202 (2009).
48. Wolfenden, R., Lewis, C. A. Jr. & Yuan, Y. Kinetic challenges facing oxalate, malonate, acetoacetate and oxaloacetate decarboxylases. *J. Am. Chem. Soc.* **133**, 5683–5685 (2011).
49. Goldstein, S. & Rabani, J. The ferrioxalate and iodide–iodate actinometers in the UV region. *J. Photochem. Photobiol. A* **193**, 50–55 (2008).
50. Sasselov, D. D., Grotzinger, J. P. & Sutherland, J. D. The origin of life as a planetary phenomenon. *Sci. Adv.* **6**, eaax3419 (2020).
51. Cleaves, H. J. II The prebiotic geochemistry of formaldehyde. *Precambrian Res.* **164**, 111–118 (2008).
52. Yew, W. S. et al. Evolution of enzymatic activities in the enolase superfamily: D-tartrate dehydratase from *Bradyrhizobium japonicum*. *Biochemistry* **45**, 14598–14608 (2006).
53. Sagi, V. N., Punna, V., Hu, F., Meher, G. & Krishnamurthy, R. Exploratory experiments on the chemistry of the 'glyoxylate scenario': formation of ketosugars from dihydroxyfumarate. *J. Am. Chem. Soc.* **134**, 3577–3589 (2012).
54. Liu, Z. et al. Harnessing chemical energy for the activation and joining of prebiotic building blocks. *Nat. Chem.* **12**, 1023–1028 (2020).

Methods

General methods. All reagents and deuterated solvents used for the reactions and spiking experiments were purchased from Sigma-Aldrich and were used without further purification. All the photochemical reactions were carried out in Norell Suprasil quartz NMR tubes purchased from Sigma-Aldrich and Hg lamps with a principal emission at 254 nm were used in a Rayonet photochemical chamber reactor RPR-200, acquired from The Southern New England Ultraviolet Company. StarLab is an in-house-constructed photoreactor that delivers broadband ultraviolet–visible irradiation (from 220 to about 750 nm by using water as an optical filter) to a sample from a 75 W xenon lamp manufactured by Horiba[38]. A Mettler Toledo SevenEasy pH Meter S20 was used to monitor the pH, and degassed H_2O or D_2O was achieved by four rounds of freeze–pump–thaw cycling. ^{1}H and ^{13}C NMR spectra were acquired using a Bruker Ultrashield 400 Plus or Bruker Ascend 400 operating at 400.1 or 100.6 MHz, respectively. Samples that consisted of H_2O/D_2O mixtures were analysed using HOD suppression to collect the ^{1}H-NMR data. Chemical shifts (δ) are shown in ppm. Coupling constants (J) are given in Hertz and the notations s, d, t represent the multiplicities singlet, doublet and triplet, respectively. The conversion yields were determined by relative integrations of the signals using a known amount of acetamide as the internal reference in the ^{1}H NMR spectrum.

General method for the photoreaction of carboxylates with sulfite. Carboxylates and sodium sulfite (final concentrations are given in Extended Data Figs. 1 and 2) were dissolved in degassed H_2O/D_2O (9:1, 0.5 ml). After the pH was adjusted to the reported value with NaOH/HCl, the mixture was transferred to a quartz NMR tube, which was sealed and irradiated for the reported time (Extended Data Figs. 1 and 2). The resultant solution was analysed by ^{1}H and/or ^{13}C NMR spectroscopy. The yield was calculated by spiking with 4,5-dicyanoimidazole (final concentration of 0.5 mM, 1 mM or 5 mM) and relative integration.

Preparing hydrogen gas in an NMR tube. Metallic zinc (~6 mg) was added to 0.5 ml of HCl (0.1 M) aqueous solution. This solution was transferred to an NMR tube after being vortexed for 5 s and then analysed by ^{1}H NMR spectroscopy.

Sulfate identification. Sodium bicarbonate (21 mg, 0.25 mmol) and sodium sulfite (63 mg, 0.5 mmol) were dissolved in degassed water (10 ml) and the pH of the resultant solution was adjusted to 9 by adding NaOH/HCl solution. The mixture was then sealed in a quartz tube and irradiated with 254 nm light in the Rayonet photoreactor for 4 h. A 3 ml aliquot of the resulting solution was diluted to 20 ml with water and acidified to pH = 1 by the addition of concentrated HCl. The acidified solution was heated to nearly boiling for at least 30 min to remove all the CO_2 and SO_2. Barium chloride solution was then added to the solution to give a precipitate, which persisted on boiling for another 30 min. The precipitate did not dissolve in dilute HCl solution (ref. [17]).

Ultrafast pump–probe experiments. The general principles of pump–probe spectroscopy are described in the literature[55–57]. The fundamental of the excitation pulses (800 nm) was generated by a Ti:Sa-based laser-amplifier system (Solstice Ace by Spectra-Physics) with a repetition rate of 1 kHz and a pulse duration of ~90 fs. The excitation pulses (251 nm) were generated in a non-linear amplifier system (Topas Prime + NIRUVis, Light Conversion, Ltd) and stretched by a 25 cm fused silica block (Corning) to ~1.7 ps to suppress two-photon ionization of the solvent. The excitation energy at the sample position was ~1 μJ with a spot diameter of ~250 μm (full-width at half-maximum). For our microsecond ultrafast pump–probe spectroscopy (Supplementary Table 2), the broadband probe light (unpolarized) was generated, delayed and detected in an EOS Fire system (Ultrafast Systems, LLC), with a nominal spectral range of 350–950 nm. For our picosecond ultrafast pump–probe spectroscopy (Supplementary Fig. 32), the broadband probe light was generated, delayed and detected in a HELIOS Fire System (Ultrafast Systems, LLC), with a nominal spectral range of 400–750 nm. These spectral ranges are ideal to monitor the broad absorption feature of the hydrated electron, which is centred near 700 nm. The experiments were carried out at a temperature of 23 °C.

The transient pump–probe data were cropped to the spectral range 450–913 nm and 20 adjacent channels were averaged (Surface Xplorer, Ultrafast Systems, LLC). A global fitting analysis to determine the transient lifetimes was performed[58–60].

Ultrafast pump–probe spectroscopic investigation of reduction chemistry. The rate constant reported in the literature for the reaction of hydrated electrons with formate **2** ($k = 2.4 \times 10^4$ M^{-1} s^{-1})[26] is considerably lower than that for the reduction of oxalate (the average of three values given in Buxton et al.[61] is 3.1×10^7 M^{-1} s^{-1}). However, in our experiments, oxalate **10** is also prone to photoionization[34,35] and so it is not clear if the reaction of hydrated electrons with oxalate in our experiments is, or is not, faster than the reaction of hydrated electrons with formate **2**. The rate constant for the reaction of hydrated electrons with glycolate **5** ($k = 8.2 \times 10^6$ M^{-1} s^{-1}) (ref. [32]) is high, although the authors of that paper caution that this "unexpectedly high value may be due to trace impurity in the sample". Furthermore, although the rate constant for the reaction of solvated electrons with CO_2 is known[23], we do not know the concentration of CO_2 in our experiments, or whether the catalysis of its interconversion with carbonic acid and bicarbonate by sulfite affects this rate. Accordingly, we used ultrafast pump–probe spectroscopy both to confirm the photoionization of oxalate **10** and compare it with that of sulfite (Supplementary Fig. 32a), and to measure the hydrated electron decay kinetics in mixtures representative of the mixtures used in our continuous irradiation experiments (Supplementary Table 3). These pump–probe experiments confirmed the photoionization of oxalate **10** and further revealed that bicarbonate, formate **2** and glycolate **5** react at similar rates with hydrated electrons in our experiments, and that oxalate **10** reacts considerably faster (Supplementary Fig. 32 and Supplementary Tables 2 and 3).

Data availability

All data generated or analysed during this study are included in the manuscript and the Supplementary Information.

References

55. Schrader, T. et al. Vibrational relaxation following ultrafast internal conversion: comparing IR and Raman probing. *Chem. Phys. Lett.* **392**, 358–364 (2004).
56. Ryseck, G. et al. The excited-state decay of 1-methyl-2(1*H*)-pyrimidinone is an activated process. *ChemPhysChem* **12**, 1880–1888 (2011).
57. Haiser, K. et al. Mechanism of UV-induced formation of Dewar lesions in DNA. *Angew. Chem. Int. Ed.* **51**, 408–411 (2012).
58. Satzger, H. & Zinth, W. Visualization of transient absorption dynamics—towards a qualitative view of complex reaction kinetics. *Chem. Phys.* **295**, 287–295 (2003).
59. Dominguez, P. N. et al. Primary reactions in photosynthetic reaction centers of *Rhodobacter sphaeroides*—time constants of the initial electron transfer. *Chem. Phys. Lett.* **601**, 103–109 (2014).
60. Gutierrez-Osuna, R., Nagle, H. T. & Schiffman, S. S. Transient response analysis of an electronic nose using multi-exponential models. *Sens. Actuators B* **61**, 170–182 (1999).
61. Buxton, G. V., Greenstock, C. L., Helman, P. & Ross, A. B. Critical review of rate constants for reactions of hydrated electrons, hydrogen atoms and hydroxyl radicals in aqueous solution. *J. Phys. Chem. Ref. Data* **17**, 513–886 (1988).

Acknowledgements

We thank the J.D.S., D.D.S. and W.W.F. group members for helpful discussions. This research was supported by the Medical Research Council (MC_UP_A024_1009 to J.D.S.), the Simons Foundation (290362 to J.D.S., 290360 to D.D.S. and 554187 to W.W.F.). C.L.K. and D.D.S. thank W. Zinth, P. Dominguez, D. Yahalomi and G. Lozano for helpful discussions and experimental assistance, and acknowledge the Harvard Origins of Life Initiative.

Author contributions

Z.L. discovered this carboxysulfitic chemistry and explored its scope under the supervision of J.D.S. and with the assistance of L.-F.W., C.L.K. performed the pump–probe experiments under the supervision of D.D.S. and W.W.F. evaluated the geochemical relevance of the chemistry. All the authors co-wrote the manuscript.

Competing interests

The authors declare no competing interests.

Additional information

Extended data is available for this paper at https://doi.org/10.1038/s41557-021-00789-w.

Supplementary information The online version contains supplementary material available at https://doi.org/10.1038/s41557-021-00789-w.

Correspondence and requests for materials should be addressed to John D. Sutherland.

Peer review information *Nature Chemistry* thanks the anonymous reviewers for their contribution to the peer review of this work.

Reprints and permissions information is available at www.nature.com/reprints.

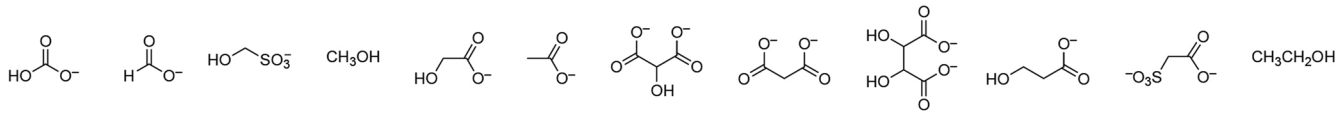

1 **2** **3** **4** **5** **6** **7** **8** **9** **11** **29** **37**

Entry	[$NaHCO_3$] /mM	[Na_2SO_3] /mM	Products												Time
			2[a]	**3**	**4**	**5**	**6**	**7**	**8**	**9a**	**9b**	**11**	**29**	**37**	
1	5	10	0.03 0.6 %			20 0.8 %	10 0.4 %	120 7.2 %	30 1.8 %						4 h
2	20	40	3.7 19 %		40 0.2 %	100 1.0 %	20 0.2 %	600 9.0 %	200 3.0 %						4 h
3	50	100	18.0 36 %	200 0.4 %	200 0.4 %	200 0.8 %	50 0.2 %	600 3.6 %	300 1.8 %	30 0.24 %	30 0.24 %				4 h
4	100	200	27.6 28 %	500 0.5 %	120 0.1 %	20 0.04 %	20 0.04 %	150 0.5 %	40 0.12 %						4 h
5[b]	100	200	52.7 53 %	200 0.2 %	4600 4.6 %	300 0.6 %	300 0.6 %	500 1.5 %	900 2.7 %	30 0.12 %	20 0.08 %	100 0.3 %			24 h
6[c]	5	4 × 10	0.03 0.6%			20 0.8%	27 1.0%	110 6.6%	270 16.2%				20 0.8%		4 x 1h
7[d]	5	50	1.6 32 %	15 0.3 %	143 2.9 %	12 0.5 %	8 0.3 %	59 3.5 %	102 6.1 %				8 0.3 %	45 1.8 %	168 h

a. Concentration of formate **2** in mM, concentrations of other products in μM. b. The experiment was repeated with ^{13}C-labelled bicarbonate, after 24 hours irradiation, the remaining bicarbonate was about 40 mM (Fig. S20). c. The concentration of sodium bicarbonate was 5 mM with 10 mM sodium sulfite initially followed by additional 10 mM sodium sulfite hourly (40 mM total). d. Using a lower intensity broadband lamp source (StarLab).

Extended Data Fig. 1 | Product concentrations and percentage yields after UV irradiation of solutions of $NaHCO_3$ and Na_2SO_3.

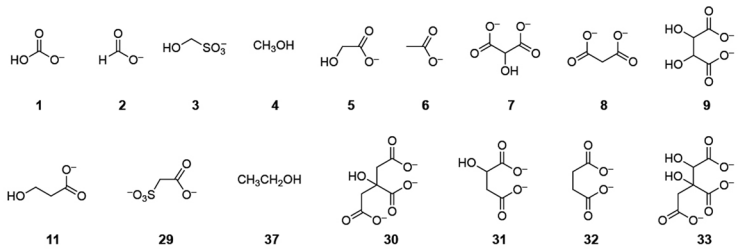

Entry	Reactant	Products																Time
		2[a]	**3**	**4**	**5**	**6**	**7**	**8**	**9a**	**9b**	**11**	**29**	**30**	**31**	**32**	**33**	**37**	
1	**2**	*32.1*[b] *64 %*	1900 3.8 %	3300 6.6 %	300 1.2 %	240 1.0 %	340 2.0 %	550 3.3 %				70 0.28 %						4 h
2	**3**	6.9 14 %	*38000*[b] *76 %*	4200 8.0 %		200 0.8 %												7 h
3	**4**	1.4 2.8 %	2300 4.6 %	*40000*[b] *80 %*		273 1.09 %											1580 6.32 %	6 h
4	**5**	0.6 0.6 %	700 0.7 %	150 0.15 %	*3500*[b] *7 %*	16200 32 %		100 0.3 %	1500[d] 6 %	1000 4 %		8000 16 %	200 1.2 %	3000 12 %	1070 4.4 %	190 1.1 %		6 h
5	**5**[c]			10 0.1 %	*940*[b] *18 %*	1000 20 %		40 1.2 %	380[d] 15 %	190 7.6%		810 16 %	15 0.9 %	390 15.6 %	70 2.8 %			2 h
6	**5**[e]	0.7 0.7 %	400 0.4 %	20 0.02 %	*42500*[b] *85 %*	1700 3.4 %			400[d] 1.6 %	400 1.6 %		200 0.4 %		200 0.8 %				8 h
7	**5**[e,f]	0.89 8.9 %	35 0.35 %	40 0.4 %	*945*[b] *19 %*	356 7.12 %		15 0.45 %	210[d] 8.4 %	105 4.2 %	50 1.5%	130 2.6 %		50 2.0 %	5 0.2%			144 h
8	**6**			40 0.04 %	100 0.2 %	*37000*[b] *74 %*		30 0.09 %				1600 3.2 %			90 0.36 %		480 0.96 %	6 h
9	**7**	2.4 1.6 %					*11200*[b] *22.4 %*	24300 48.6 %	N.d.[g]	120 0.3 %	800 1.6 %	400 0.5 %						7 h
10	**8**	0.4 0.3 %				200 0.3 %		*46000*[b] *92 %*			2000 4.0 %							2 h
11	**10**	9.2 9.2 %		40 0.04 %	3700 7.4 %	100 0.2 %	200 6.0 %	50 0.15 %	1100 4.4 %	1100 4.4 %				300 1.2 %				6 h

a. Concentration of product formate **2** in mM, concentrations of other products in μM. b. The concentration and percentage of remaining starting material. c. The concentration of glycolate **5** was 5 mM with 10 mM sodium sulfite. d. The total yields of **7** and **9a**, because the siganls are obscured. e. Using a lower intensity broadband lamp source (StarLab). f. The concentration of glycolate **5** was 5 mM with 50 mM sodium sulfite. g. Not distinguishable, ^{1}H-NMR signal obscured by the signal for starting material **7**.

Extended Data Fig. 2 | Product concentrations and percentage yields after irradiation of individual bicarbonate reduction products (50 mM) and Na_2SO_3 (100 mM).